

# Effect of size, temperature and strain rate on dislocation density and deformation mechanisms in Cu nanowires

P. Rohith<sup>a,b</sup>, G. Sainath<sup>b,\*</sup>, V.S. Srinivasan<sup>a,c</sup>

<sup>a</sup>Homi Bhabha National Institute (HBNI), Indira Gandhi Centre for Atomic Research, Kalpakkam, Tamilnadu-603102, India

<sup>b</sup>Materials Development and Technology Division, Metallurgy and Materials Group, Indira Gandhi Centre for Atomic Research, Kalpakkam, Tamilnadu-603102, India

<sup>c</sup>Scientific Information Resource Division, Resource Management & Public Awareness Group, Indira Gandhi Centre for Atomic Research, Kalpakkam, Tamilnadu-603102, India

---

## Abstract

In the present study, molecular dynamics (MD) simulations have been performed to understand the effect of nanowire size, temperature and strain rate on the variations in dislocation density and deformation mechanisms in  $\langle 100 \rangle$  Cu nanowires. The nanowire size has been varied in the range 1.446-43.38 nm with a constant length of 21.69 nm. Different temperatures varying from 10 K to 700 K and strain rates in the range of  $5 \times 10^7 - 1 \times 10^9 \text{ s}^{-1}$  have been considered. For all the conditions, the variations in dislocation density ( $\rho$ ) has been calculated as a function of strain. The results indicate that the variations in dislocation density exhibits two stages irrespective of the conditions: (i) dislocation exhaustion at small strains followed by (ii) dislocation starvation at high strains. However, with decreasing size and increasing temperature, the rate of dislocation exhaustion increases, which results in early transition from dislocation exhaustion stage to dislocation starvation stage. Similarly, with increasing strain rate, the rate of dislocation exhaustion and also the transition strain increases.

*Keywords:* Molecular Dynamics simulations; Cu nanowire; Dislocation density; Dislocation exhaustion; Dislocations starvation.

---

## 1. Introduction

Technological advancements have paved the way towards the development of nanocomponents in nanoelectro mechanical systems (NEMS). Nano components used in NEMS are required to withstand the complex stress state with minimal probability of failure. Hence, it is important to understand the mechanical properties such as strength and associated deformation mechanisms like dislocation density. Generally, the mechanical properties of nanowires are determined using nanoindentation tests, while tensile tests are most common in bulk materials. However, performing experiments at nanoscale involves many complications. Alternatively, molecular dynamics (MD) simulations provide great insights in determining mechanical

---

\*Corresponding author

Email address: [sg@igcar.gov.in](mailto:sg@igcar.gov.in) (G. Sainath)

properties and understanding the deformation behaviour of nanowires with atomic-scale resolution.

Plastic deformation in bulk materials is characterized by dislocation multiplication, dislocation pile-up, dislocation cross-slip and similar processes, which leads to strain hardening/softening before final failure. However, in nanomaterials, dislocations can travel limited distances before annihilating at free surfaces/grain boundaries, thereby reducing the probability of dislocation multiplication [1, 2]. The strengthening behavior in the bulk materials with respect to grain size can be described by the well known Hall-Petch relation. A physical basis for this behavior is associated with the difficulty of dislocation movement across grain boundaries and the stress concentration arising due to dislocation pile-up [3, 4]. However, as the grain size decreases to nanoscale regime, the grain boundary volume fraction increases significantly and as a result, the grain boundary mediated processes such as GB sliding and GB rotation becomes more important [3, 4]. In particular, when the grain size is reduced to below certain critical size, the strength of materials decreases with decreasing grain size, i.e., it follows inverse HallPetch relation. In the absence of grain boundaries in single crystalline nanowires, the surface alone influences the strength and deformation mechanisms [5]. In nanowires, the strength increases with decreasing size, which is mainly attributed to surface effects. Contrary to nanowires, the surface effects are absent in bulk single crystals. These differences suggests that the deformation mechanisms governing the plastic deformation in nanomaterials/nanowires are quite different from their bulk counterparts. Since then, many researchers have proposed different mechanisms such as source exhaustion and source truncation, dislocation exhaustion, dislocation starvation, and weakest link theory to understand the deformation behaviour at nanoscale [6, 7, 8, 9, 10, 11, 12, 13, 14, 15, 16]. These mechanisms originate from either micro-structural parameters or dimensional constraints. Oh et al. [11] had performed in-situ tensile tests on Al single crystals and observed the operation of single ended dislocation sources without any multiplication mechanism. Greer et al. [6] have performed the compression tests on Au nanopillars and reported that the dislocations would leave the pillars before they multiply, leading to dislocation starvation. Once nanopillar is in dislocation-starved state, very high stresses are required to nucleate new dislocations, either at surfaces or in the interior [6]. Parthasarathy et al. [8] have reported that the reduction in nanowire size transforms the double ended Frank-Read sources into single ended sources leading to increased strength by source truncation. Volkert and Lilleodden [7] have shown that the image stresses due to surfaces and source limited behaviour results in dislocation annihilation at free surface. This leads to dislocation starvation resulting in increase strength for activation of dislocation sources at smaller sizes. Sansoz [13] had performed MD simulations on compressive loading of Cu nanopillars with initial dislocation density. It has been demonstrated that the deformation exhibits a pronounced dislocation exhaustion regime followed by source limited activation regime. El-Alwady [14] had studied the effect of sample size and initial dislocation density on deformation mechanisms. It was reported that dislocation starvation is dominant in small size nanowires. However, in relatively larger size, with increasing initial dislocation density, the dominant deformation mechanism changes from dislocation starvation to single-source mechanism and then to dislocation exhaustion and finally forest hardening [14]. Further, it was

mentioned that as sample size increases, dislocation density at which the deformation mechanisms transits decreases. However, all these studies were mainly focussed on size related effects on deformation mechanisms and little has been studied about the combined influence of size, temperature and strain rate. Particularly, the influence of temperature and strain rate on the variations in dislocation density and also on deformation mechanisms such as dislocation exhaustion and dislocation starvation has not been investigated. In view of this, effect of size, temperature and strain rate on deformation mechanisms of  $\langle 100 \rangle$  Cu nanowire has been investigated in the present study using MD simulations. The variation of dislocation density as a function of strain has been calculated for all the scenarios. Based on the variations in dislocation density, two type of deformation mechanisms (dislocation exhaustion and dislocation starvation) have been identified.

## 2. MD Simulation details

Cu nanowires of square cross-section shape oriented in  $\langle 100 \rangle$  direction with  $\{001\}$  as side surfaces were chosen for the present study. In order to study the influence of size, nanowires of different size varying from 1.446 to 43.38 nm, all having a constant length of 21.69 nm were used. Periodic boundary conditions were chosen along length direction, while other two directions were kept free to mimic an infinitely long nanowire. On these nanowires, tensile loading was simulated using MD simulations through LAMMPS package [17]. Embedded atom method (EAM) potential for FCC Cu given by Mishin and co-workers [18] has been used to describe the inter-atomic interactions. This potential has been chosen for being able to reproduce the stacking fault and twinning fault energies of Cu [19], which are important to predict the dislocation related mechanisms.

Following the initial construction of nanowires, energy minimization was performed by conjugate gradient method to obtain a stable structure. Velocity verlet algorithm was used to integrate the equations of motion with a time step of 2 fs. Finally, the relaxed model was thermally equilibrated to required temperature in NVT ensemble with a Nose-Hoover thermostat. This configuration of nanowire has been taken as initial state for further tensile simulations. Following thermal equilibration, nanowires were subjected to tensile loading along axial direction at required temperature and strain rate. MD simulations have been performed at various temperatures in the range 10 -700 K and strain rates varying from  $5 \times 10^7$  to  $1 \times 10^9$  s<sup>-1</sup>. These strain rates are significantly higher than the experimental strain rates. However, despite the high strain rates, many studies have shown that MD simulation results are in good agreement with the experimental investigations. The average stress in loading direction has been calculated using Virial expression [20] as implemented in LAMMPS. The dislocations in present study have been identified/tracked by using Dislocation eXtraction Algorithm (DXA) developed by Stukowski [21] as implemented in OVITO [22]. The detailed procedure for tracking the dislocation lines and their Burgers vectors is provided in the paper [21]. Following the detection of dislocation lines, the total length of dislocation lines within the simulated volume can be obtained in OVITO. In the present study, we have considered all type of dislocations (Shockley partials, full dislocations, Frank partials and stair rods) while calculating the total length. Once the total length is obtained, the

dislocation density has been calculated as the total dislocation length divided by simulated cell volume. This procedure has been repeated for every 250 time steps (0.5 ps).

### 3. Results and Discussion

Figure 1 shows the variations in dislocation density along with flow stress as a function of strain under tensile loading of a nanowire with size  $(d) = 21.69$  nm and strain rate of  $1 \times 10^9$  s<sup>-1</sup> at 10 K. It can be seen that the nanowire undergoes elastic deformation up to a peak followed by an abrupt drop in flow stress. This abrupt drop is associated with yielding through the nucleation of  $1/6\langle 112 \rangle$  Shockley partial dislocations in the nanowire. During the process of this yielding, large number of dislocations nucleate and as a result, the dislocation density reaches its maximum value (Figure 1). With increasing deformation, dislocation density gradually decreases from its maximum until a strain value of 0.56. This regime, where dislocation density gradually decreases is denoted as dislocation exhaustion stage. Interestingly, this exhaustion stage is associated with slight increase in flow stress (Figure 1). Since the deformation in nanowires is nucleation controlled [23], decrease in dislocation density indicates that the rate of exhaustion or annihilation is higher than the nucleation. Following dislocation exhaustion stage, dislocation density remains very low and constant with marginal fluctuations around a mean value (Figure 1). This low value of dislocation density indicates that the nanowire is depleted of dislocations, and therefore, this regime ( $\varepsilon > 0.56$ ) is termed as dislocation starvation stage. In starvation stage, deformation proceeds through continuous nucleation and annihilation of dislocations, which is also reflected in terms of fluctuations in dislocation density as well as flow stress (Figure 1). Further, the marginal fluctuations at low and constant value of dislocation density indicates that the rate of dislocation nucleation is almost same as the rate of dislocation annihilation. Finally, it can be seen that the dislocation density during the deformation of nanowire is in the range of  $1 \times 10^{16} - 6 \times 10^{17}$  m<sup>-2</sup> (Figure 1), which is few orders of magnitude higher than those observed in experiments. However, many MD simulation studies have reported such high values of dislocation density, which is attributed to high applied strain rates inherent in MD [15, 16, 24, 25, 26, 27].

In order to investigate the influence of size, temperature and strain rate on the variations in dislocation exhaustion and starvation stages, the dislocation density as a function of strain (or time) has been calculated for all the cases. Figure 2a shows the variations in dislocation density as a function of strain (or time) for Cu nanowires of different cross-section width in the range 1.446-43.38 nm and strain rate of  $1 \times 10^9$  s<sup>-1</sup> at 10 K. Dislocation density is shown only up to a strain level of 1 as it remains almost constant above this level. It can be seen that for all sizes except the smallest, dislocation density exhibits two stages; dislocation exhaustion stage followed by dislocation starvation stage (Figure 2a). In the smallest nanowire, large fluctuations around low value of dislocation density suggest that there is no dislocation exhaustion stage and dislocation starvation alone dominates the deformation at all strains. Further, the transition strain at which the dislocation mechanism changes from exhaustion stage to starvation stage increases with increasing size. This indicates that the rate of dislocation exhaustion is higher in small size nanowires. The

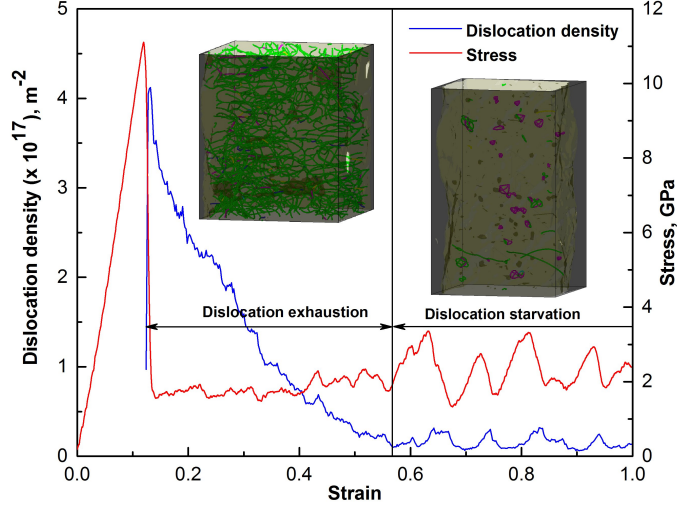


Figure 1: Variations in dislocation density along with flow stress as a function of strain at 10 K and strain rate of  $1 \times 10^9 \text{ s}^{-1}$  for a nanowire of size ( $d$ ) = 21.69 nm. The regions of dislocation exhaustion and starvation are clearly marked. In the inset figures, the green colour lines show  $1/6\langle 112 \rangle$  partials and the magenta lines indicate stair-rod dislocations.

rate of dislocation exhaustion is calculated as a slope of dislocation density vs. time plot as typically shown in Figure 2a for nanowire of size 43.38 nm. Figure 2b shows the variation of dislocation exhaustion rate as a function of nanowire size. It can be clearly seen that, the rate of dislocation exhaustion ( $\dot{\rho}$ ) decreases with increasing size ( $d$ ) (Figure 2b) and follows the relation  $\dot{\rho} = \rho_{d0} + ae^{-bd}$ , where  $\rho_{d0}$ ,  $a$ , and  $b$  are constants. The high exhaustion rates or low resident time of dislocations in small size nanowires is due to many factors like lower probability of dislocation-defect interactions and high image stresses. On the contrary, the high probability of dislocation-defect interactions and low image stress results in low rate of dislocation exhaustion in large nanowires (Figure 2b).

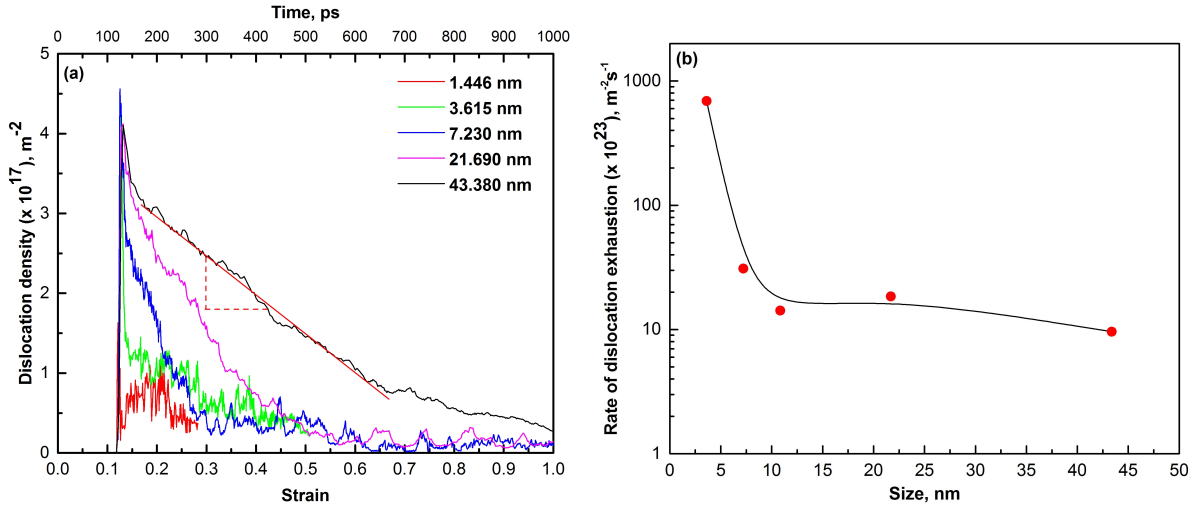


Figure 2: (a) Variations in dislocation density as a function of strain (or time) for nanowires of different size deformed at a constant strain rate of  $1 \times 10^9 \text{ s}^{-1}$  and temperature of 10 K. (b) The variations in rate of dislocation exhaustion with respect to nanowire size.

The variations in dislocation density for a nanowire of size ( $d$ ) = 10.85 nm as a function of strain (or time) at different temperatures are shown in Figure 3a at a constant strain rate of  $1 \times 10^9 \text{ s}^{-1}$ . At all temperatures, dislocation density in nanowires clearly display dislocation exhaustion and starvation stages. Further, with increasing temperature, the maximum in dislocation density, which is observed at yielding, decreases (Figure 3a), while the rate of dislocation exhaustion increases (Figure 3b). The rate of dislocation exhaustion ( $\dot{\rho}$ ) with temperature ( $T$ ) follows the relation  $\dot{\rho} = \rho_{T0} - ae^{-bT}$ , where  $\rho_{T0}$ ,  $a$ , and  $b$  are constants. The high dislocation exhaustion rates at high temperatures results in low values of transition strain for change in deformation mechanisms from exhaustion to starvation. The low exhaustion rates at low temperatures are due to high dislocation density at yielding (Figure 3a) and low velocity of dislocations [28], which increases the probability of dislocation interactions. The high probability of dislocation interactions restricts the ease of dislocation annihilation to surfaces resulting in low exhaustion rates at low temperatures.

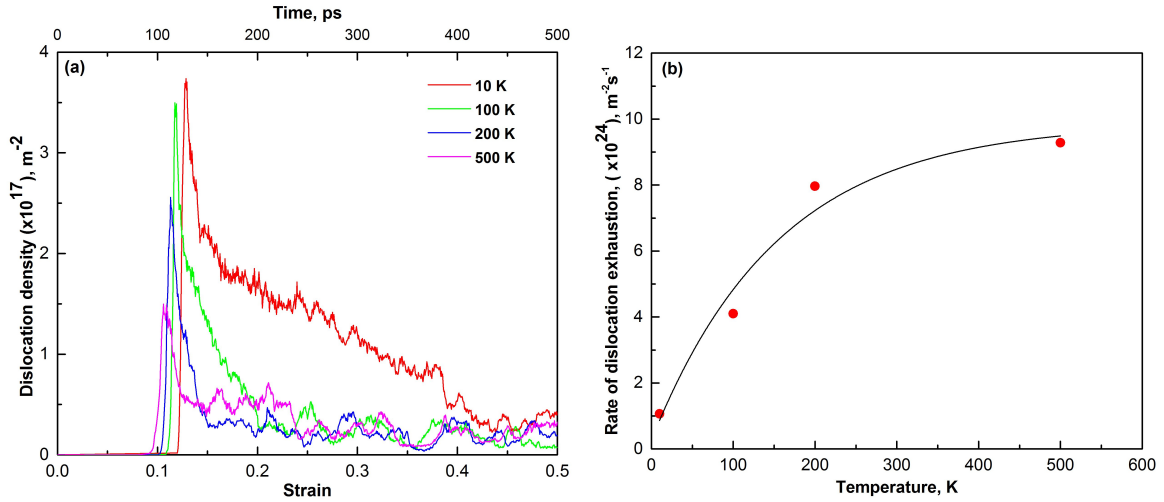


Figure 3: (a) Variations in dislocation density as a function of strain (or time) at different temperatures for a nanowire of size ( $d$ ) = 10.85 nm deformed at a constant strain rate of  $1 \times 10^9 \text{ s}^{-1}$ . (b) The variations in dislocation exhaustion rates as a function of temperature.

Figure 4a shows the variations in different dislocation mechanisms (dislocation exhaustion and starvation stages) as a function of strain at different strain rates for a nanowire of size ( $d$ ) = 10.85 nm at 10 K. Due to different applied strain rates, which results in different time scales, the time axis has not shown in Figure 4a. Similar to size and temperature, it shows that the strain rate also influences the dislocation mechanisms in Cu nanowires. It can be seen that, with increasing strain rates, both maximum dislocation density at yielding and transition strain (exhaustion to starvation) increases (Figure 4a). However, unlike size and temperature cases, the variations in dislocation density show different behaviour with respect to strain and time. With respect to strain (Figure 4a), it appears that the dislocations exhaust at low rates under high strain rate conditions. However, this is not actually true when the calculations are obtained from dislocation density vs. time. This difference with respect to strain and time is due to different time scales involved at different strain rates. For example, under high strain rate condition, it takes very short time to reach the strain value

of 0.5, while it takes longer time to reach the same strain value under low strain rate case. Interestingly, the results obtained from dislocation density vs. time graph show that the dislocation exhaustion rate increases with increasing strain rate as shown in Figure 4b and follows the relation  $\dot{\rho} = \rho_{\varepsilon 0} - ae^{-b\varepsilon}$ , where  $\rho_{\varepsilon 0}$ ,  $a$ , and  $b$  are constants. Since the dislocation velocity is directly proportional to strain rate [29], high exhaustion rates are expected under high strain rate conditions.

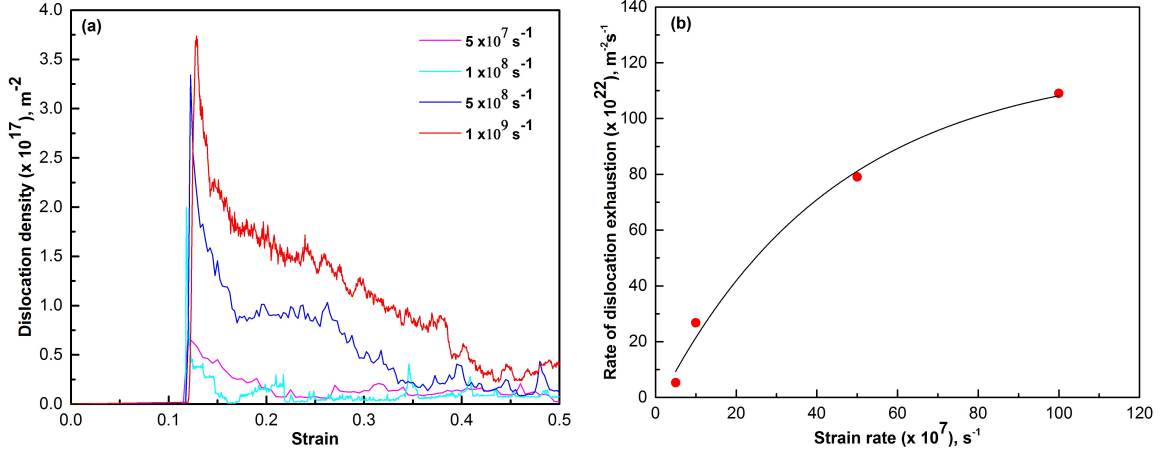


Figure 4: (a) Variations in dislocation density as a function of strain at different strain rates for a nanowire of size ( $d$ ) = 10.85 nm deformed at 10 K. (b) The variations in dislocation exhaustion rate as a function of strain rates.

The dislocation density influences the different properties of materials, out of which the most prominent being the mechanical properties. In bulk materials increasing the dislocation density increases the yield strength, which results in work hardening [29]. Similarly, the variations in dislocation density in the nanowires has many consequences on strength, ductility and deformation mechanisms [16, 30]. For example, it has been shown that the yield stress is very sensitive to initial dislocation density [30]. In a crystal with low initial dislocation density, the nucleation and growth of twins along with strain hardening has been reported, whereas in crystal with high initial dislocation density, the deformation proceeds by dislocation multiplication and motion without any twins and exhibit no strain hardening [30]. Further, it has been shown that the nanowires with high dislocation density display large ductility as compared to nanowires with low dislocation density [16]. This has been attributed to high dislocation-dislocation interactions in nanowires containing high dislocation density.

#### 4. Conclusions

MD simulations were used to understand the variations in dislocation density as a function of strain for different nanowire sizes, temperatures and strain rates. The results indicate that, irrespective of temperature and strain rate, the dislocation density in all the nanowires except with  $d = 1.446$ , show two stage behaviour; dislocation exhaustion stage at small strains followed by dislocation starvation stage at large strains. However, small size nanowires with  $d < 3.615$  nm exhibit only dislocation starvation at all strains. Further, in

all the cases, the dislocation density attains its maximum immediately after yielding. During dislocation exhaustion, it has been observed that the rate of dislocation exhaustion strongly depends on nanowire size, temperature and strain rate. The large size nanowires show lower exhaustion rates as compared to smaller ones, i.e., resident time of dislocations within the nanowire increases with increasing size. The lower exhaustion rates in large size nanowires are due to high probability of dislocation-defect interactions along with low image stress. As a result of low exhaustion rates, large size nanowires show higher transition strain (strain to change in dislocation mechanisms from exhaustion to starvation) as compared to small size nanowires. Similarly, in nanowire of particular size, the dislocation exhaustion rates increases with increasing temperature and strain rate. Correspondingly, the transition strain decreases with increasing temperature and decreasing strain rate. The lower exhaustion rates at low temperatures and low strain rates are mainly due to low dislocation velocities, which increases the probability of dislocation interactions with existing defects or dislocations and thus restricting the ease of dislocation annihilation to surfaces.

## References

- [1] J.J. Gilman, *Appl. Micromech. Flow Solids*, (1953) 185.
- [2] R. Krahne, L. Manna, G. Morello, A. Figuerola, C. George, S. Deka, *Nano Sci. Tech.*, Springer, New York, 2013.
- [3] L. Zhang, C. Lu, K. Tieu, *Comput. Mater. Sci.* 118 (2016) 180.
- [4] L. Zhang, Y. Shibuta, X. Huang, C. Lu, M. Liu, *Comput. Mater. Sci.* 156 (2019) 421.
- [5] C. R. Weinberger and W. Cai, *J. Mater. Chem.*, 22 (2012) 3277.
- [6] J.R. Greer, W.C. Oliver, W.D. Nix, *Acta Mater.* 53 (2005) 1821.
- [7] C.A. Volkert and E.T. Lilleodden, *Philos. Mag.* 86 (2006) 5567.
- [8] T.A. Parthasarathy, S.I. Rao, D.M. Dimiduk, M.D. Uchic, D.R. Trinkle, *Scr. Mater.* 56 (2007) 313.
- [9] S.I. Rao, D.M. Dimiduk, M. Tang, T.A. Parthasarathy, M.D. Uchic, C. Woodward, *Philos. Mag.* 87 (2007) 4777.
- [10] M.D. Uchic, P.A. Shade, and D.M. Dimiduk, *Annu. Rev. Mater. Res.* 39 (2009) 361.
- [11] S.H. Oh, M. Legros, D. Kiener, and G. Dehnm, *Nat. Mater.* 8 (2009) 95.
- [12] O. Kraft, P. Gruber, R. Monig, and D. Weygand, *Annu. Rev. Mater. Res.* 40 (2010) 293.
- [13] F. Sansoz, *Acta Mater.* 59 (2011) 3364.
- [14] J.A. El-alwady, *Nat. Commun.* 6 (2015) 5926.
- [15] M. Yaghoobi and G.Z. Voyiadjis, *Acta Mater.* 121 (2016) 190.
- [16] G. Sainath, P. Rohith, and B.K. Choudhary, *Philos. Mag.* 97 (2017) 2632.



- [17] S. Plimpton, *J. Comp. Phy.* 117 (1995) 1.
- [18] Y. Mishin, M.J. Mehl, D.A. Papaconstantopoulos, A.F. Voter, and J.D. Kress, *Phys. Rev. B* 63 (2001) 1.
- [19] W. Liang and M. Zhou, *Phys. Rev. B* 73 (2006) 115409.
- [20] J.A. Zimmerman, E.B. Webb, J.J. Hoyt, R.E. Jones, P.A. Klein, and D.J. Bammann, *Modell. Simul. Mater. Sci. Eng.* 12 (2003) S319.
- [21] A. Stukowski and K. Albe, *Modell. Simul. Mater. Sci. Eng.* 18 (2010) 025016.
- [22] A. Stukowski, *Modell. Simul. Mater. Sci. Eng.* 18 (2010) 015012.
- [23] D. Mordehai, O. David, and R. Kositski, *Adv. Mater.* (2018) 1706710.
- [24] S.W. Lee S.M. Han, and W.D. Nix, *Act Mater.* 57 (2009) 4404.
- [25] A.T. Jennings, M.J. Burek, and J.R. Greer, *Phys. Rev. Lett.* 104 (2010) 135503.
- [26] K. Kolluri, M.R. Gungor, and D. Maroudas, *J. Apply. Phys.* 105 (2009) 093515.
- [27] S. Mojumder, *Physica B: Condensed Matter* 530 (2018) 86.
- [28] A.P.L. Turner and T. Vreeland Jr., *Acta Metall.* 18 (1970) 1225.
- [29] G.E. Dieter and D.J. Bacon, *Mechanical metallurgy*, McGraw-hill, New York, Vol. 3, 1986.
- [30] L.A. Zepeda-Ruiz, A. Stukowski, T. Ooppelstrup, and V.V. Bulatov, *Nature* 550 (2017) 492.